Flow of gaseous mixtures through rectangular microchannels driven by pressure, temperature, and concentration gradients

S. Naris and D. Valougeorgis
Department of Mechanical and Industrial Engineering, University of Thessaly, Pedion Areos, Volos 38334, Greece

D. Kalempa and F. Sharipov
Departamento de Física, Universidade Federal do Paraná, Caixa Postal 19044, Curitiba 81531-990, Brazil

The flow of binary gaseous mixtures through rectangular microchannels due to small pressure, temperature, and molar concentration gradients over the whole range of the Knudsen number is studied. The solution is based on a mesoscale approach, formally described by two coupled kinetic equations, subject to diffuse scattering boundary conditions. The model proposed by McCormack substitutes the complicated collision term and the resulting kinetic equations are solved by an accelerated version of the discrete velocity method. Typical results are presented for the flow rates and the heat fluxes of two different binary mixtures (Ne–Ar and He–Xe) with various molar concentrations, in two-dimensional microchannels of different aspect (height to width) ratios. The formulation is very efficient and can be used instead of the classical method of solving the Navier–Stokes equations with slip boundary conditions, which is restricted by the hydrodynamic regime. Moreover, the present formulation is a good alternative to the direct simulation Monte Carlo method, which often becomes computationally inefficient. © *2005 American Institute of Physics*. [DOI: 10.1063/1.1896986]

I. INTRODUCTION

The development of new technologies in the fabrication of microsized mechanical parts and equipment has a major impact on many disciplines including fluid dynamics and transport phenomena.[1] When dealing with flows in the scale of microns or smaller, many unexpected phenomena have been observed. The flow characteristics at the macro and micro levels are not the same and the features of micromechanics require additional basic and applied research work.

In most cases, these problems have been studied by either direct simulation Monte Carlo on the microlevel[2–4] or by adding correction terms to the continuum equations at the macrolevel.[5–7] In the first approach, a motion of huge number of model particles interacting between them and with solid surfaces is considered. Such calculations require large computer memory and long CPU time. The second approach is based on the velocity slip and temperature jump boundary conditions[8–11] applied to the Navier–Stokes equations. This method requires less computational effort but it is restricted to moderately small Knudsen numbers, say $Kn \leqslant 1$.

An alternative methodology to calculate the transport phenomena in microchannels over the whole range of the Knudsen number with modest computational effort is based on the Boltzmann equation[12–14] or simplified kinetic models,[15] where the basic unknown is the particle distribution function. The macroscopic quantities of practical interest are readily obtained by taking moments of the distribution function.

Such a kinetic approach to rarefied gas flows is very well known and it is successfully used during the last decades to calculate gas flows in vacuum systems. The main results on these flows are resumed in the review.[15] From the mathematical viewpoint, gas flows in microfluidics and in other types of micro electro-mechanical systems (MEMS) are exactly the same as those in vacuum systems. So, the data summarized in Ref. 15 can be directly applied to microflows over the whole range of the gas rarefaction. Of course, numerical solutions of the kinetic equations are more complicated than those of the hydrodynamic equations. However nowadays, it is easy to solve directly the kinetic equations due to the availability of high speed computers and due to the significant advancement in the computational kinetic theory made during the last years.

Internal rarefied gaseous flows of a single gas in one dimension has been extensively studied over the last several decades and a number of interesting phenomena, which vanish at the continuum limit, have been revealed.[15] This theory has been extended to single gas flows through two dimension rectangular channels, see Refs. 16–18. However, in practice one deals with gaseous mixtures more often than with a single gas. In spite of their great practical importance, the gaseous mixture flows have received less attention because of their complexity. It is noted that in gaseous mixtures new transport phenomena appear, i.e., mass and heat fluxes due to the imposed concentration gradient and diffusion due to the imposed pressure, temperature, and concentration gradients. Also in gaseous mixtures, the required computational effort drastically increases, due to a large number of parameters (molecular masses and diameters, intermolecular forces, concentration, gas-surface accommodation coefficients) involved in the calculations. Such a complexity explains the

17, 100607-1

fact that most of the previous works on internal rarefied gas mixture flows are limited to problems with plane and axisymmetric geometric configurations.[19–22] Recently, the binary gaseous mixture flow between two plates has been studied in a more detailed and systematic manner, see Refs. 23–28, applying the McCormack model.[29] During the course of these recent works, it has been found that this kinetic model provides accurate results with much less computational effort than the Boltzmann equation used for the same problems in Refs. 30 and 31.

Very recently, applying the McCormack model, the flow of gaseous mixtures through a 2D rectangular duct due to an imposed pressure gradient has been solved.[32] Here, this work is extended to the more general problem of a gas mixture flow due to pressure, temperature, and concentration gradients in the longitudinal direction of a rectangular channel. The solution of the coupled kinetic equations is obtained using an accelerated version of the discrete velocity method.[33] The formulation is very efficient and the solution is accurate and valid in the whole range of the gas rarefaction. Therefore, the proposed methodology is more general than the widely used method of solving the continuum equations with the slip boundary conditions, which, in any case, is restricted by the hydrodynamic regime.

II. STATEMENT OF THE PROBLEM

Consider a flow of a binary gaseous mixture through a long microchannel with a constant cross section restricted as $-H/2 \leq x' \leq H/2$ and $-W/2 \leq y' \leq W/2$ (H is the channel height and W is its width). Without loss of generality, the height is assumed to be smaller or equal to the width of the channel ($H \leq W$). The flow is caused by longitudinal small gradients of pressure, temperature, and concentration defined as

$$X_P = \frac{H}{P}\frac{\partial P}{\partial z'}, \quad X_T = \frac{H}{T}\frac{\partial T}{\partial z'}, \quad X_C = \frac{H}{C}\frac{\partial C}{\partial z'}, \tag{1}$$

respectively. Here, z' is the longitudinal coordinate, while P, T, and C are pressure, temperature, and molar concentration of the mixture in a given cross section. The smallness of the gradients means that

$$|X_P| \ll 1, \quad |X_T| \ll 1, \quad |X_C| \ll 1. \tag{2}$$

The molar concentration is defined as

$$C = \frac{n_1}{n_1 + n_2}, \tag{3}$$

where n_α, $\alpha=1$, 2 is the number density of gaseous species α. We neglect the end effects and consider only the longitudinal components of the hydrodynamic velocity and heat flow vectors, which are functions of the transverse coordinates, i.e.,

$$\mathbf{u}' = [0,0,u'(x',y')] \tag{4}$$

and

$$\mathbf{q}' = [0,0,q'(x',y')]. \tag{5}$$

In this case the shear stress tensor Π'_{ij} has the nonzero elements Π'_{xz} and Π'_{yz}, and their symmetric counterparts.

The quantities of practical interest include the mass flow rate, the heat flux, and the diffusion flux given by

$$J_M = \int_{-W/2}^{W/2}\int_{-H/2}^{H/2} \varrho u'(x',y')dx'dy', \tag{6}$$

$$J_Q = \int_{-W/2}^{W/2}\int_{-H/2}^{H/2} q'(x',y')dx'dy', \tag{7}$$

and

$$J_D = \int_{-W/2}^{W/2}\int_{-H/2}^{H/2} \varrho_1(u_1' - u')dx'dy'$$
$$= \int_{-W/2}^{W/2}\int_{-H/2}^{H/2} \frac{\varrho_1\varrho_2}{\varrho}(u_1' - u_2')dx'dy', \tag{8}$$

respectively. Here, ϱ is the mass density of the mixture

$$\varrho = \varrho_1 + \varrho_2, \tag{9}$$

$\varrho_\alpha = n_\alpha m_\alpha$ is the mass density of each species and m_α ($\alpha=1$, 2) denotes the molecular mass. The hydrodynamic velocity of the mixture is defined as

$$u' = \frac{1}{\varrho}(\varrho_1 u_1' + \varrho_2 u_2'), \tag{10}$$

where u_1' and u_2' are the bulk velocities of each species. It is also convenient to introduce the mean velocity of the mixture

$$w = \frac{1}{n}(n_1 u_1' + n_2 u_2') \tag{11}$$

and the so-called peculiar heat flow

$$q* = q' - \frac{5}{2}P(w - u'). \tag{12}$$

The aim of the present work is to calculate the flow rate of the mixture, the heat flux, and the diffusion flux over the whole range of the rarefaction parameter defined as

$$\delta = \frac{HP_0}{\mu}\sqrt{\frac{m}{2kT_0}}, \tag{13}$$

where P_0 and T_0 are the equilibrium pressure and temperature of the mixture, respectively, μ is the stress viscosity coefficient of the mixture at temperature T_0 and k is the Boltzmann constant. The mean molecular mass m of the mixture is given by

$$m = C_0 m_1 + (1 - C_0)m_2, \tag{14}$$

where

$$C_0 = \frac{n_{01}}{n_{01} + n_{02}} \tag{15}$$

is the equilibrium molar concentration and m_a and n_{0a} denote the molecular mass and equilibrium number density of each species, respectively. Considering that the viscosity μ is proportional to the molecular mean free path λ, one can see that

the rarefaction parameter δ is proportional to the inverse Knudsen number defined as $Kn = \lambda/H$.

III. GOVERNING EQUATIONS

It is convenient to introduce the dimensionless coordinates defined as

$$x = x'/H, \quad y = y'/H, \quad z = z'/H. \tag{16}$$

Next, because of the smallness of the thermodynamic forces given by Eq. (2), the Boltzmann equation can be linearized in a standard manner by representing the distribution function of each species as

$$f_\alpha(x,y,z,\mathbf{c}_\alpha) = f_\alpha^{(M)}(z,\mathbf{c}_\alpha)[1 + h_\alpha(x,y,\mathbf{c}_\alpha)], \quad |h_\alpha| \ll 1, \tag{17}$$

where $\mathbf{c}_\alpha = (c_{\alpha x}, c_{\alpha y}, c_{\alpha z})$ is the dimensionless molecular velocity, $h_\alpha(x,y,\mathbf{c}_\alpha)$ is the perturbation function of each species and

$$f_\alpha^{(M)}(z,\mathbf{c}) = n_\alpha(z)\left[\frac{m_\alpha}{2\pi k T(z)}\right]^{3/2} \exp\left[-\frac{c_\alpha^2}{T(z)/T_0}\right] \tag{18}$$

is the local Maxwellian distribution. Then the system of the kinetic Boltzmann equations for the unknown perturbation functions, in dimensionless form, reads[29]

$$c_{\alpha x}\frac{\partial h_\alpha}{\partial x} + c_{\alpha y}\frac{\partial h_\alpha}{\partial y} = \omega_\alpha \sum_{\beta=1}^{2} \hat{L}_{\alpha\beta} h_\alpha - c_{\alpha z}\left[X_P + \eta_\alpha X_c \right.$$
$$\left. + \left(c_\alpha^2 - \frac{5}{2}\right)X_T\right], \tag{19}$$

where $\alpha = 1, 2$ and

$$\omega_\alpha = H\sqrt{m_\alpha/2kT_0}, \tag{20}$$

and

$$\eta_1 = 1, \quad \eta_2 = C_0/(1 - C_0). \tag{21}$$

The collision term is the one proposed by McCormack[29] and for the problem under consideration is summarized in the Appendix. A more detailed description may be found in Refs. 22 and 29.

The dimensionless moments of the perturbation function given by

$$u_\alpha(x,y) = \frac{1}{\pi^{3/2}}\sqrt{\frac{m}{m_\alpha}}\int c_{\alpha z} h_\alpha \exp(-c_\alpha^2)d\mathbf{c}_\alpha, \tag{22}$$

$$q_\alpha(x,y) = \frac{1}{\pi^{3/2}}\sqrt{\frac{m}{m_\alpha}}\int c_{\alpha z}\left(c_\alpha^2 - \frac{5}{2}\right)h_\alpha \exp(-c_\alpha^2)d\mathbf{c}_\alpha, \tag{23}$$

and

$$\Pi_{\alpha j z}(x,y) = \frac{1}{\pi^{3/2}}\int c_{\alpha z} c_{\alpha j} h_\alpha \exp(-c_\alpha^2)d\mathbf{c}_\alpha, \quad j = x,y \tag{24}$$

are related to the hydrodynamic velocity, the heat flux, and the shear stress tensor, respectively.

Since Eq. (19) is linear, its solution can be decomposed as[22]

$$h_\alpha = h_\alpha^{(P)}X_P + h_\alpha^{(T)}X_T + h_\alpha^{(C)}X_C \tag{25}$$

and, consequently, the moments of the distribution function can also split into three independent parts:

$$u_\alpha = u_\alpha^{(P)}X_P + u_\alpha^{(T)}X_T + u_\alpha^{(C)}X_C, \tag{26}$$

$$q_\alpha = q_\alpha^{(P)}X_P + q_\alpha^{(T)}X_T + q_\alpha^{(C)}X_C, \tag{27}$$

and

$$\Pi_{\alpha j z} = \Pi_{\alpha j z}^{(P)}X_P + \Pi_{\alpha j z}^{(T)}X_T + \Pi_{\alpha j z}^{(C)}X_C, \quad j = x,y. \tag{28}$$

The dimensionless velocity and heat flow profiles, given by Eqs. (22) and (23) are integrated over the cross section of the duct to yield the reduced mass flow rate

$$U_\alpha^{(i)} = -2\frac{H}{W}\int_{-W/2H}^{W/2H}\int_{-1/2}^{1/2} u_\alpha^{(i)}(x,y)dx\,dy \tag{29}$$

and the reduced heat flux

$$Q_\alpha^{(i)} = -2\frac{H}{W}\int_{-W/2H}^{W/2H}\int_{-1/2}^{1/2} q_\alpha^{(i)}(x,y)dx\,dy, \tag{30}$$

for $\alpha = 1, 2$ and $i = P, T, C$. In the present work, Eq. (19), subject to diffuse scattering boundary conditions is solved numerically, using an accelerated discrete velocity methodology,[33] for the whole range of the rarefaction parameter δ and various values of the aspect ratio H/W. The velocity, heat flow, and stress profiles given by Eqs. (22)–(24) for each imposed thermodynamic force, as well as the mass and heat fluxes given by Eqs. (29) and (30), are calculated.

IV. THE ONSAGER–CASIMIR RELATIONS

In Refs. 34–36 the Onsager–Casimir reciprocity relations were obtained in general form for rarefied gas flows without the local equilibrium principle, i.e., for the whole range of the gas rarefaction. In the case of gaseous mixture flowing through tubes and 1D channels these relations are given in Refs. 22,26, respectively. Here we repeat only the key elements of this thermodynamic analysis, properly modified for the case of the 2D rectangular channel flow.

It has been shown that although the fluxes J_M, J_Q, and J_D, defined by Eqs. (6)–(8) linearly depend on the thermodynamic forces X_P, X_T, and X_C the kinetic coefficients of these equations do not satisfy the Onsager–Casimir reciprocity relations. However, the reciprocity relations are fulfilled when the following thermodynamic fluxes are introduced:[36]

$$J_P = -n_0\int_{-W/2}^{W/2}\int_{-H/2}^{H/2} w\,dx'dy', \tag{31}$$

$$J_T = -\frac{1}{kT_0}\int_{-W/2}^{W/2}\int_{-H/2}^{H/2} q*\,dx'dy', \tag{32}$$

$$J_C = -n_{01} \int_{-W/2}^{W/2} \int_{-H/2}^{H/2} (u_1' - u_2') dx' dy'. \tag{33}$$

Then the thermodynamic fluxes are related to the thermodynamic forces in the matrix form

$$\begin{pmatrix} J_P \\ J_T \\ J_C \end{pmatrix} = \begin{pmatrix} \Lambda'_{PP} & \Lambda'_{PT} & \Lambda'_{PC} \\ \Lambda'_{TP} & \Lambda'_{TT} & \Lambda'_{TC} \\ \Lambda'_{CP} & \Lambda'_{CT} & \Lambda'_{CC} \end{pmatrix} \begin{pmatrix} X_P \\ X_T \\ X_C \end{pmatrix}. \tag{34}$$

Since all thermodynamic forces considered here do not change their own sign under the time reversal the Onsager–Casimir relations take the form

$$\Lambda'_{PT} = \Lambda'_{TP}, \quad \Lambda'_{PC} = \Lambda'_{CP}, \quad \Lambda'_{TC} = \Lambda'_{CT}. \tag{35}$$

All kinetic coefficients have the same dimension and for further derivations it is convenient to use the reduced coefficients in the form

$$\Lambda_{ij} = \frac{2}{n_0 HW} \sqrt{\frac{m}{2kT_0}} \Lambda'_{ij}. \tag{36}$$

Thus, once the set of coefficients $\Lambda_{ij}(i, j = P, T, C)$ is known, the fluxes J_P, J_T, and J_C can be easily calculated via Eq. (34). Then, the fluxes J_M, J_Q, and J_D, which are of practical interest, can be deduced from the expressions

$$J_M = -mJ_P + (m_2 - m_1)(1 - C_0)J_C, \tag{37}$$

$$J_Q = -kT_0 \left[J_T + \frac{5}{2} \frac{m_2 - m_1}{m} (1 - C_0)J_C \right], \tag{38}$$

$$J_D = -\frac{m_1 m_2}{m}(1 - C_0)J_C. \tag{39}$$

The coefficients Λ_{ij} are calculated via the reduced mass flow, heat flux, and diffusion flux of the mixture as

$$\Lambda_{Pj} = C_0 U_1^{(j)} + (1 - C_0) U_2^{(j)}, \tag{40}$$

$$\Lambda_{Tj} = C_0 Q_1^{(j)} + (1 - C_0) Q_2^{(j)}, \tag{41}$$

and

$$\Lambda_{Cj} = C_0 [U_1^{(j)} - U_2^{(j)}], \tag{42}$$

where $j = P, T, C$. The quantities Λ_{ij} are called "reduced kinetic coefficients."[22,26] The first index i, which may be P, T, or C denotes mass flow, heat flux, and diffusion flux, respectively, while the second index j denotes the imposed thermodynamic force, which is due to a pressure P, temperature T, or concentration C gradient. The coefficients $\Lambda_{PP}, \Lambda_{TT}$, and Λ_{CC} correspond to the so-called direct effects, while the coefficients Λ_{ij} with $i \neq j$, correspond to the so-called cross effects. Since they obey the Onsager–Casimir reciprocity relations, given by Eq. (35), the total number of unknowns is reduced from nine to six.

V. THE NUMERICAL SCHEME

The discretizations in the phase (particle velocity) and physical space are based on the discrete velocity method[15] and the diamond difference scheme,[37] respectively. Since the flow is considered as fully developed in the longitudinal direction, first the c_z component of the molecular velocity is eliminated by a projection of Eq. (19) in the (c_x, c_y) phase plane. All related integrals are approximated using Gauss quadratures. For the discretization in the physical space the cross section of the duct is divided in K rectangular elements and then the continuous equations are discretized at the center of each element. The first derivatives in x and y in Eq. (19) are approximated by centered finite differences in the corresponding direction and then all terms are interpolated in terms of the corresponding quantities at the edges of each element using weighted averages. When the weights are equal, the scheme is known as the diamond difference scheme and the spatial discretization is second-order accurate.[37]

As it is well known, when the rarefaction parameter δ is large (or the Kn number is small) the convergence rate of the discrete velocity method is very slow. Also, the large number of iterations may result to accumulated round-off error. For these cases a synthetic accelerated algorithm of the discrete velocity method has been developed recently to reduce significantly the required number of iterations and to ensure accurate results.[32,33] It is noted that synthetic acceleration schemes have been applied extensively over the years to speed up the slow convergence rates in the solutions of the neutron and radiative transport equations, with dramatic theoretical and practical success.[38] It turns out that these acceleration schemes, with certain modifications, can also be applied with the same success in the iterative solution of kinetic model equations in rarefied gas dynamics.[33] The acceleration scheme is based on the formulation of moment equations, the so-called "synthetic equations," which are solved coupled with the kinetic equation to improve significantly the slow iterative convergence rate of the kinetic equation. This improvement reduces significantly the required CPU time and it is particularly important in multidimensional problems. In the present work the accelerated version of the discrete velocity method[33] is implemented in all cases with $\delta > 1$.

TABLE I. The quantities $U_{fm}, \Lambda_{PP}^{(h)}$, and $\Lambda_{PP}^{(s)}$ vs H/W.

	H/W		
	1	0.5	0.1
U_{fm}	0.8387	1.152	1.991
$\Lambda_{PP}^{(h)}$	0.0703	0.1143	0.1562
$\Lambda_{PP}^{(s)}$	0.5623	0.7492	0.9493

TABLE II. Kinetic coefficient Λ_{PP} for Ne–Ar ($C_0=0.5$) and various H/W.

δ		Λ_{PP}		
	$H/W=1$	$H/W=0.5$	$H/W=0.1$	$H/W=0$
0	8.756(-1)	1.203	2.079	∞
0.001	8.739(-1)	1.200	2.063	4.487
0.01	8.648(-1)	1.183	1.990	3.207
0.1	8.300(-1)	1.123	1.748	2.137
1	8.012(-1)	1.086	1.484	1.600
10	1.341	1.988	2.640	2.805
50	4.115	6.514	8.818	9.397

TABLE IV. Kinetic coefficient Λ_{CC} for Ne–Ar ($C_0=0.5$) and various H/W.

δ		Λ_{CC}		
	$H/W=1$	$H/W=0.5$	$H/W=0.1$	$H/W=0$
0	8.756(-1)	1.203	2.079	∞
0.001	8.734(-1)	1.199	2.060	4.474
0.01	8.601(-1)	1.174	1.965	3.142
0.1	7.881(-1)	1.048	1.571	1.880
1	5.266(-1)	6.342(-1)	7.520(-1)	7.837 (-1)
10	1.297(-1)	1.343(-1)	1.379(-1)	1.388 (-1)
50	2.902(-2)	2.922(-2)	2.936(-2)	2.942 (-2)

VI. FREE MOLECULAR AND HYDRODYNAMIC REGIMES

In the free molecular regime every gaseous species flows independently to each other. In this case the solution for a single gas[17] can be used. Then, the kinetic coefficients read

$$\Lambda_{PP} = U_{fm}\left[C_0\left(\frac{m}{m_1}\right)^{1/2} + (1-C_0)\left(\frac{m}{m_2}\right)^{1/2} \right], \quad (43)$$

$$\Lambda_{TT} = \frac{9}{4}\Lambda_{PP}, \quad (44)$$

$$\Lambda_{CC} = C_0 U_{fm}\left[\left(\frac{m}{m_1}\right)^{1/2} + \frac{C_0}{(1-C_0)}\left(\frac{m}{m_2}\right)^{1/2} \right], \quad (45)$$

$$\Lambda_{PT} = \Lambda_{TP} = -\frac{1}{2}\Lambda_{PP}, \quad (46)$$

$$\Lambda_{PC} = \Lambda_{CP} = C_0 U_{fm}\left[\left(\frac{m}{m_1}\right)^{1/2} - \left(\frac{m}{m_2}\right)^{1/2} \right], \quad (47)$$

and

$$\Lambda_{TC} = \Lambda_{CT} = -\frac{1}{2}\Lambda_{PC}, \quad (48)$$

where

$$U_{fm} = \frac{1}{\sqrt{\pi}}\frac{H}{W}\int_{-W/2H}^{W/2H}\int_{-1/2}^{1/2}\left[\left(\frac{W}{2H}-y\right)\ln\left(\frac{1+\sin\varphi}{1-\sin\varphi}\right) \right. $$
$$\left. + \left(\frac{1}{2}-x\right)\ln\left(\frac{1+\cos\varphi}{1-\cos\varphi}\right) \right]dx\,dy, \quad (49)$$

with

$$\varphi = \arctan\left(\frac{1/2-x}{W/2H-y}\right). \quad (50)$$

The numerical values of U_{fm} are calculated in Ref. 17 and are given in Table I, for specific values of the aspect ratio.

In the hydrodynamic regime the kinetic coefficient Λ_{PP} may be split in two parts as

$$\Lambda_{PP} = \delta\Lambda_{PP}^{(h)} + \sigma_P\Lambda_{PP}^{(s)}. \quad (51)$$

The first term is calculated from the analytical solution of the Navier–Stokes equation with non-slip boundary conditions to yield

$$\Lambda_{PP}^{(h)} = \frac{1}{6}\left[1 - 192\frac{H}{W}\sum_{i=0}^{\infty}\frac{1}{n^5}\tanh\left(\frac{nW}{2H}\right) \right], \quad n = \pi(2i+1). \quad (52)$$

The second term of Eq. (51) is obtained as the slip correction to this analytical solution and it contains the viscous slip coefficient σ_P calculated in Ref. 23 for several mixtures. Both $\Lambda_{PP}^{(h)}$ and $\Lambda_{PP}^{(s)}$ do not depend on the chemical composition of mixture and the data obtained in Ref. 17 for a single gas can be used for any mixture. Numerical values of $\Lambda_{PP}^{(h)}$ and $\Lambda_{PP}^{(s)}$ are given in Table I for the specific aspect ratios.

The other kinetic coefficients, i.e., $\Lambda_{TT}, \Lambda_{CC}, \Lambda_{PT}, \Lambda_{PC}, \Lambda_{TC}$ do not depend on the aspect ratio because they are calculated as mean values of the bulk velocities $u_\alpha^{(T)}, u_\alpha^{(C)}$, and heat flux $q_\alpha^{(C)}$, which are constant over the cross section of the channel in the hydrodynamic regime. So, the analytical expressions,

TABLE III. Kinetic coefficient Λ_{TT} for Ne–Ar ($C_0=0.5$) and various H/W.

δ		Λ_{TT}		
	$H/W=1$	$H/W=0.5$	$H/W=0.1$	$H/W=0$
0	1.970	2.706	4.677	∞
0.001	1.965	2.697	4.632	1.007(1)
0.01	1.933	2.639	4.411	7.083
0.1	1.768	2.350	3.530	4.269
1	1.197	1.455	1.758	1.844
10	3.296(-1)	3.450(-1)	3.573(-1)	3.605(-1)
50	7.664(-2)	7.736(-2)	7.790(-2)	7.812(-2)

TABLE V. Kinetic coefficient Λ_{TP} for Ne–Ar ($C_0=0.5$) and various H/W.

δ		$-\Lambda_{TP}(=-\Lambda_{PT})$		
	$H/W=1$	$H/W=0.5$	$H/W=0.1$	$H/W=0$
0	4.378(-1)	6.014(-1)	1.039	∞
0.001	4.359(-1)	5.980(-1)	1.024	1.950
0.01	4.259(-1)	5.797(-1)	9.521(-1)	1.313
0.1	3.816(-1)	5.039(-1)	7.153(-1)	7.706 (-1)
1	2.661(-1)	3.249(-1)	3.717(-1)	3.800 (-1)
10	9.113(-2)	9.686(-2)	1.009(-1)	1.019 (-1)
50	2.301(-2)	2.337(-2)	2.365(-2)	2.372 (-2)

TABLE VI. Kinetic coefficient Λ_{CP} for Ne–Ar ($C_0=0.5$) and various H/W.

	$\Lambda_{CP}(=\Lambda_{PC})$			
δ	$H/W=1$	$H/W=0.5$	$H/W=0.1$	$H/W=0$
0	1.480(−1)	2.034(−1)	3.514(−1)	∞
0.001	1.478(−1)	2.030(−1)	3.496(−1)	8.146 (−1)
0.01	1.463(−1)	2.001(−1)	3.387(−1)	5.842 (−1)
0.1	1.360(−1)	1.816(−1)	2.810(−1)	3.540 (−1)
1	8.936(−2)	1.073(−1)	1.310(−1)	1.382 (−1)
10	1.891(−2)	1.934(−2)	1.977(−2)	1.987 (−2)
50	3.983(−3)	3.998(−3)	4.025(−3)	3.995 (−3)

TABLE VIII. Kinetic coefficient Λ_{PP} for He–Xe ($C_0=0.5$) and various H/W.

	Λ_{PP}			
δ	$H/W=1$	$H/W=0.5$	$H/W=0.1$	$H/W=0$
0	2.025	2.781	4.807	∞
0.001	2.022	2.776	4.779	1.091(1)
0.01	2.004	2.743	4.637	7.872
0.1	1.914	2.584	4.056	5.124
1	1.649	2.159	2.885	3.106
10	1.698	2.403	3.121	3.302
50	4.296	6.738	9.088	9.680

$$\Lambda_{TT} = \frac{\varrho}{\mu}\left[\kappa\frac{T_0}{P_0} + C_0(1-C_0)\alpha_T^2 D_{12}\right]\frac{1}{\delta}, \tag{53}$$

$$\Lambda_{CC} = \frac{C_0 \varrho D_{12}}{(1-C_0)\mu}\frac{1}{\delta}, \tag{54}$$

$$\Lambda_{PT} = \Lambda_{TP} = \left[\frac{n_{01}(1-C_0)D_{12}\alpha_T}{\mu}(m_2-m_1) - \sigma_T\right]\frac{1}{\delta}, \tag{55}$$

$$\Lambda_{PC} = \Lambda_{CP} = \left[\frac{n_{01}D_{12}}{\mu}(m_2-m_1) - \sigma_C\right]\frac{1}{\delta}, \tag{56}$$

and

$$\Lambda_{TC} = \Lambda_{CT} = \frac{n_{01}mD_{12}\alpha_T}{\mu}\frac{1}{\delta}, \tag{57}$$

obtained in Ref. 26 for a channel with $H/W=0$ can be used for any aspect ratio.

The expressions for the kinetic coefficients obtained in this section can be used to test the numerical solution near the free molecular and hydrodynamic regimes.

VII. RESULTS AND DISCUSSION

The numerical results presented here refer to the noble gaseous mixtures of Ne–Ar and He–Xe, with various molar concentrations. The molecular masses of these species are 4.0026, 20.183, 39.948, and 131.3 in atomic units for He, Ne, Ar, and Xe, respectively. Thus, the present study includes one mixture with species of molecular masses close to each other and another one with species of quite different masses.

The calculations have been carried out over the wide range of the rarefied parameter $10^{-3} \leqslant \delta \leqslant 50$ with the aspect ratios $H/W=1$, 0.5, and 0.1 and various equilibrium molar concentrations C_0. It is useful to remind that due to the definition of the molar concentration, higher values of C_0, correspond to higher values of n_{01}, which is taken always to be the lighter species.

To calculate the quantities $\nu_{\alpha\beta}^{(i)}$ in Eqs. (A1)–(A3), the omega integrals $\Omega_{kl}^{(ij)}$ must be given, which depend on the intermolecular interaction law. It has been shown[26] that the hard-sphere model does not provide reliable results when mixture flow problems are studied. For that reason the omega integrals obtained from experimental data on the transport coefficients in Ref. 39 were used assuming the temperature $T=300$ K.

The grid in the physical space is taken 101×101 for $\delta \leqslant 1$ and 301×301 for $\delta>1$. These phase and physical space discretizations have been found adequate to have reliable results up to at least four significant figures, with a relative convergence criterion of the iterative scheme equal to 10^{-6}. The accuracy of the numerical results has been verified in several ways. In all cases tested we have verified the Onsager–Casimir reciprocity relations within the accuracy of the numerical results. Also when we allow our data to reduce to the case of a single gas, by taking $m_1=m_2$ and $d_1=d_2$, the well known results based on the Bhatnagar-Gross-Krook and S models are recovered.[17,18] In addition, for very small values of the aspect ratio our results tend to the corresponding 1D results.[26] Finally, we have verified that for all cases tested our computational results confirm the identity

TABLE VII. Kinetic coefficient Λ_{CT} for Ne–Ar ($C_0=0.5$) and various H/W.

	$-\Lambda_{CT}=(-\Lambda_{TC})$			
δ	$H/W=1$	$H/W=0.5$	$H/W=0.1$	$H/W=0$
0	7.403(−2)	1.017(−1)	1.757(−1)	∞
0.001	7.387(−2)	1.014(−1)	1.743(−1)	3.586 (−1)
0.01	7.288(−2)	9.957(−2)	1.667(−1)	2.480 (−1)
0.1	6.739(−2)	8.979(−2)	1.333(−1)	1.487 (−1)
1	4.658(−2)	5.620(−2)	6.513(−2)	6.700 (−2)
10	1.136(−2)	1.170(−2)	1.196(−2)	1.203 (−2)
50	2.494(−3)	2.509(−3)	2.518(−3)	2.523 (−3)

TABLE IX. Kinetic coefficient Λ_{TT} for He–Xe ($C_0=0.5$) and various H/W.

	Λ_{TT}			
δ	$H/W=1$	$H/W=0.5$	$H/W=0.1$	$H/W=0$
0	4.556	6.258	1.082(1)	∞
0.001	4.547	6.243	1.074(1)	2.451 (1)
0.01	4.492	6.141	1.034(1)	1.754 (1)
0.1	4.180	5.590	8.602	1.083 (1)
1	2.981	3.675	4.577	4.856
10	9.254(−1)	9.814(−1)	1.027	1.039
50	2.258(−1)	2.286(−1)	2.308(−1)	2.316 (−1)

TABLE X. Kinetic coefficient Λ_{CC} for He–Xe ($C_0=0.5$) and various H/W.

| δ | Λ_{CC} | | | |
	$H/W=1$	$H/W=0.5$	$H/W=0.1$	$H/W=0$
0	2.024	2.781	4.807	∞
0.001	2.021	2.776	4.777	1.090(1)
0.01	2.000	2.736	4.620	7.824
0.1	1.884	2.530	3.924	4.919
1	1.429	1.784	2.237	2.369
10	4.772(−1)	5.055(−1)	5.282(−1)	5.340(−1)
50	1.155(−1)	1.169(−1)	1.179(−1)	1.183(−1)

TABLE XII. Kinetic coefficient Λ_{CP} for He–Xe ($C_0=0.5$) and various H/W.

| δ | $\Lambda_{CP}=(\Lambda_{CP})$ | | | |
	$H/W=1$	$H/W=0.5$	$H/W=0.1$	$H/W=0$
0	1.423	1.954	3.378	∞
0.001	1.421	1.951	3.359	7.783
0.01	1.407	1.926	3.258	5.613
0.1	1.329	1.786	2.789	3.541
1	1.007	1.257	1.588	1.688
10	3.267(−1)	3.452(−1)	3.606(−1)	3.645(−1)
50	7.781(−2)	7.864(−2)	7.931(−2)	7.948(−2)

$$C_0\left(\frac{\partial\Pi_{1xz}}{\partial x}+\frac{\partial\Pi_{1yz}}{\partial y}\right)+(1-C_0)\left(\frac{\partial\Pi_{2xz}}{\partial x}+\frac{\partial\Pi_{2yz}}{\partial y}\right)$$
$$=X_P+C_0X_C, \qquad (58)$$

which expresses the momentum conservation law. Most of the verifications have been performed by two different computer codes, implementing the typical discrete velocity method and its accelerated version.

The reduced kinetic coefficients Λ_{ij} for the two mixtures under investigation are tabulated in Tables II–XIII in terms of the rarefaction parameter δ for $C_0=0.5$ and for three different values of the aspect ratio. It is noted that for a given value of δ, as the aspect ratio is decreased, the channel cross section is increased, since the height is kept constant and the width is increased. Thus as the aspect ratio goes to zero, we obtain the 1D channel results for the corresponding value of δ, which are also shown in Tables II–XIII. The negative sign at some of the kinetic coefficients corresponding to cross effects, imply that in these cases, there is a mass flow or a heat flux opposite to the main flow or flux due to the imposed thermodynamic force (gradient). For example, the negative sign in front of Λ_{PT} and Λ_{CT}, implies that the flows caused by the temperature gradient are directed from a lower temperature to a higher one, which are known as thermal creep and thermal diffusion (or Soret effect) flows, respectively.

In general, the 2D duct flow results given in Tables II–XIII, have a qualitative behavior similar to those of the single gas case,[17,18] i.e., in all cases considered here, Λ_{PP} has the so-called Knudsen minimum at $\delta\sim1$, while all other coefficients decrease by increasing the rarefaction parameter δ

and, finally, vanish at the hydrodynamic limit ($\delta\to\infty$). By comparing the results given in Tables II–VII with the corresponding ones given in Tables VIII–XIII, it can be seen that the absolute values of all kinetic coefficients of the He–Xe mixture are considerably higher than those of the Ne–Ar mixture and more specifically the values of Λ_{CP} and Λ_{CT} are higher about one order of magnitude. This is due to the fact that the He–Xe mixture, compared to the Ar–Ne mixture, has a larger molecular mass ratio. So, the chemical composition of mixture affects strongly the quantitative behavior of the kinetic coefficients.

By comparing the present results with those reported in the preceding paper[26] we conclude that near the hydrodynamic regime all kinetic coefficients except Λ_{PP} are very close to those obtained for the 1D flow, i.e., at $H/W=0$. In accordance to Eqs. (53)–(57) all coefficients (except Λ_{PP}) do not depend on the aspect ratio in the hydrodynamic regime, i.e., at $\delta\to\infty$, while in the transition and free molecular regimes they depend significantly on the aspect ratio. From Tables II–XIII it can be seen that by increasing the aspect ratio all kinetic coefficients decrease drastically. Approximately, we may say that when $0.5\geqslant H/W\geqslant1$ the values of all kinetic coefficients, except Λ_{PP}, remain about a constant value for $10^{-3}\leqslant\delta\leqslant10^{-1}$, they decrease linearly to $\ln\delta$ for $10^{-1}\leqslant\delta\leqslant10$ and, finally, they tend to zero for $\delta>10$.

The behavior of the kinetic coefficients in terms of the molar concentration C_0 for both mixtures is shown in Figs. 1–3 for $\delta=0.01$, 1 and 10, respectively. It is noted that the values of the kinetic coefficients $\Lambda_{CC},\Lambda_{CP}$ (or Λ_{PC}), and Λ_{CT} (or Λ_{TC}) at $C_0=1$ must be considered as limit values because

TABLE XI. Kinetic coefficient Λ_{TP} for He–Xe ($C_0=0.5$) and various H/W.

| δ | $-\Lambda_{TP}=(-\Lambda_{TP})$ | | | |
	$H/W=1$	$H/W=0.5$	$H/W=0.1$	$H/W=0$
0	1.012	1.390	2.403	∞
0.001	1.009	1.385	2.377	4.777
0.01	9.912(−1)	1.352	2.246	3.274
0.1	9.023(−1)	1.197	1.751	1.941
1	6.286(−1)	7.678(−1)	8.925(−2)	9.143(−1)
10	2.029(−1)	2.151(−1)	2.234(−2)	2.254(−1)
50	5.122(−2)	5.203(−2)	5.266(−2)	5.283(−2)

TABLE XIII. Kinetic coefficient Λ_{CT} for He–Xe ($C_0=0.5$) and various H/W.

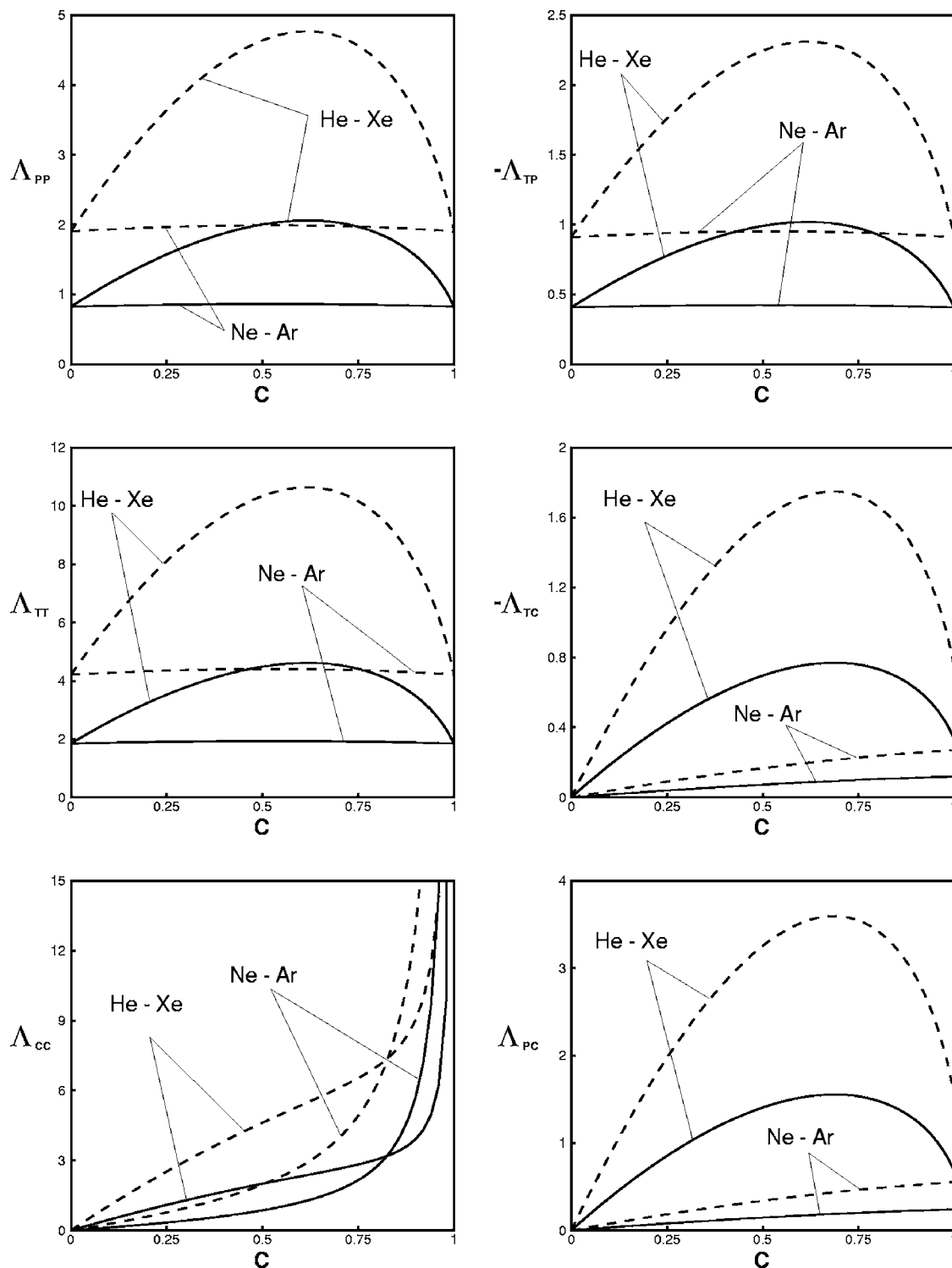| δ | $-\Lambda_{CT}=(-\Lambda_{TC})$ | | | |
	$H/W=1$	$H/W=0.5$	$H/W=0.1$	$H/W=0$
0	7.114(−1)	9.772(−1)	1.689	∞
0.001	7.094(−1)	9.737(−1)	1.672	3.418
0.01	6.977(−1)	9.521(−1)	1.587	2.354
0.1	6.368(−1)	8.456(−1)	1.247	1.397
1	4.346(−1)	5.272(−1)	6.155(−1)	6.329(−1)
10	1.160(−1)	1.200(−1)	1.230(−1)	1.238(−1)
50	2.575(−2)	2.590(−2)	2.601(−2)	2.607(−2)

FIG. 1. Kinetic coefficients vs C_0 for $\delta=0.01$ (solid line, $H/W=1$; dashed line, $H/W=0.1$).

in this case the first component of the mixture is single and the corresponding phenomena do not exist. In other words, the limit values correspond to a concentration very close but not equal to 1. It is seen that the variation of C_0 has a small effect on the results in the case of the Ne–Ar mixture, which has a molecular mass ratio $m_{Ar}/m_{Ne} \simeq 2$, while it has a much more significant effect on the results of the He–Xe mixture, which has a molecular mass ratio $m_{Xe}/m_{He} \simeq 33$. Actually,

for the Ne–Ar mixture, the coefficients $\Lambda_{PP}, \Lambda_{TT}$, and Λ_{PT} (or Λ_{TP}) have a very small variation for $0 \leqslant C_0 \leqslant 1$. The coefficient Λ_{CC} is the one with the strongest dependency on C_0 and it increases by increasing the concentration of the lighter component. In the case of the He–Xe mixture the dependency of the results on C_0 is strong and the peak values of the kinetic coefficients (except Λ_{CC}) occurs around $C_0=0.7$ in all presented cases.
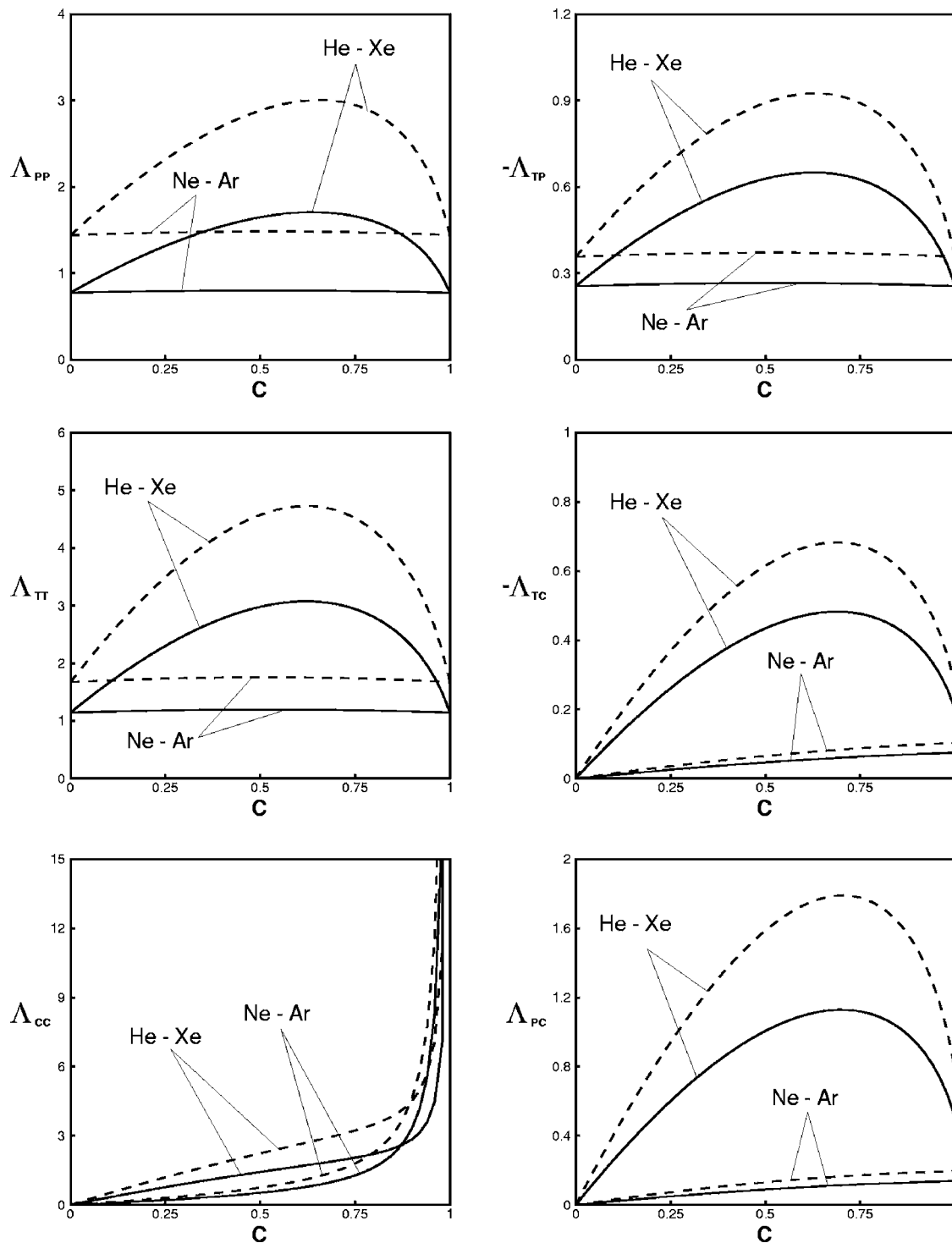
FIG. 2. Kinetic coefficients vs C_0 for $\delta=1$ (solid line, $H/W=1$; dashed line, $H/W=0.1$).

VIII. CONCLUDING REMARKS

The general flow problem of binary gaseous mixtures through rectangular microchannels due to small pressure, temperature, and molar concentration gradients over the whole range of the Knudsen number has been solved implementing a mesoscale kinetic approach. The kinetic equations based on the model proposed by McCormack, have been solved by an accelerated version of the discrete velocity method. A complete set of results has been provided for the flow rates and the heat fluxes of two gas mixtures (Ne–Ar and He–Xe), with quite different molecular mass ratio. The effects of the mixture molar concentration and of the aspect ratio (height to width) of the microchannel on the mass and heat fluxes have been investigated in detail. It will be seen in future work if the numerical results, can be parametrized to provide general algebraic expressions valid for a wide class of noble gas mixtures.
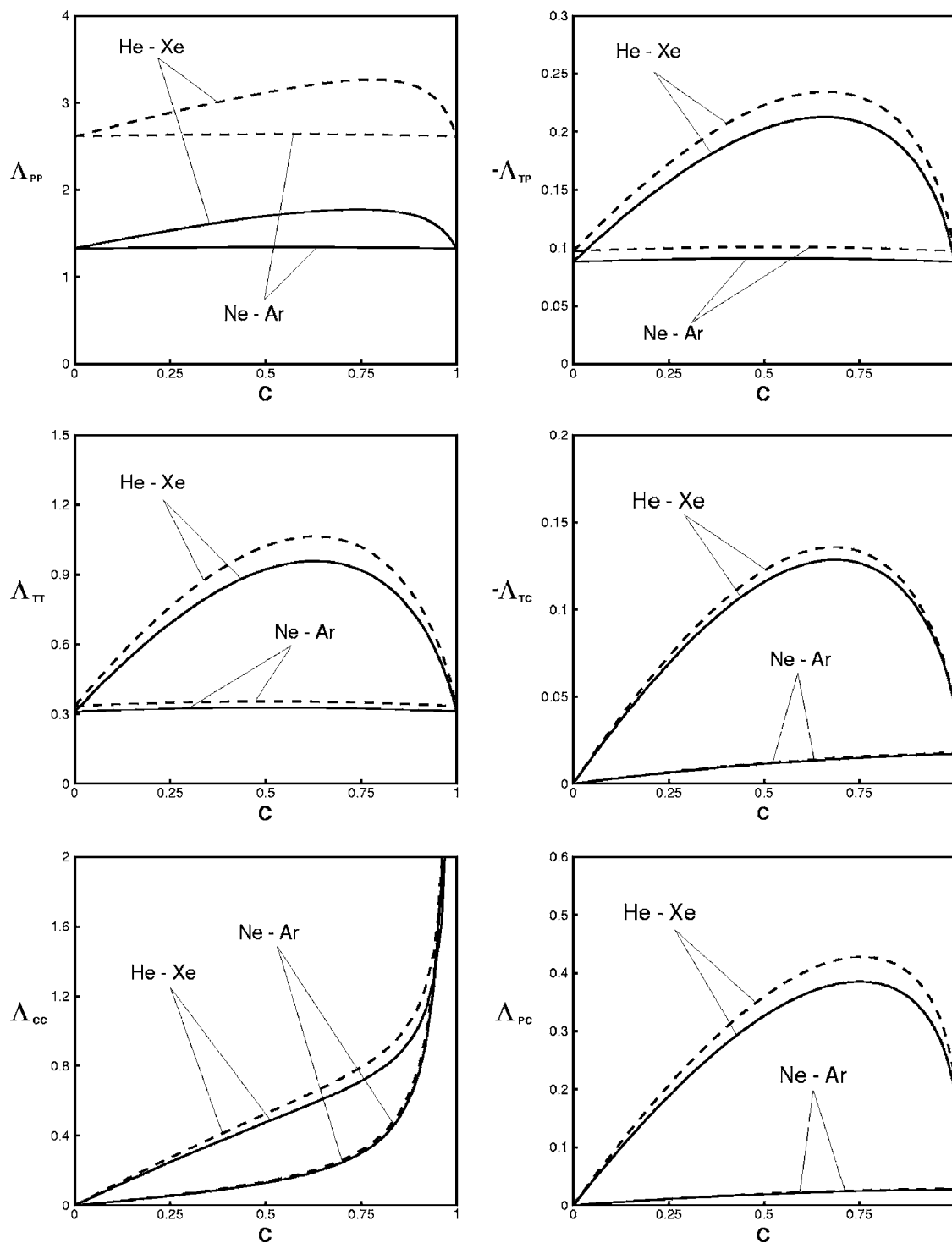
FIG. 3. Kinetic coefficients vs C_0 for $\delta = 10$ (solid line, $H/W = 1$; dashed line, $H/W = 0.1$).

The efficient and accurate formulation presented here can be implemented with modest computational effort for any binary gaseous mixture to provide reliable results for the whole range of the gas rarefaction in an unique manner. The proposed methodology must be used instead of the more common approach, which is based on the Navier–Stokes equations with slip boundary conditions, which is, in any case, restricted by the hydrodynamic regime. This is important for microflow simulations in MEMS applications, especially when the characteristic size of the microflow is comparable to the molecular mean free path.

APPENDIX: BASIC ELEMENTS OF THE McCORMACK LINEARIZED COLLISION TERM

The McCormack linearized collision term[29] for the flow problems under consideration reads

$$
\hat{L}_{\alpha\beta}h_\alpha = -\gamma_\alpha h_\alpha + 2\sqrt{\frac{m_\alpha}{m}}\left[\gamma_\alpha u_\alpha - \nu^{(1)}_{\alpha\beta}(u_\alpha - u_\beta) - \frac{1}{2}\nu^{(2)}_{\alpha\beta}\right.
$$
$$
\times\left(q_\alpha - \frac{m_\alpha}{m_\beta}q_\beta\right)\right]c_{\alpha z} + 4[(\gamma_{\alpha\beta} - \nu^{(3)}_{\alpha\beta})\Pi_{\alpha xz}
$$
$$
+ \nu^{(4)}_{\alpha\beta}\Pi_{\beta xz}]c_{\alpha z}c_{\alpha x} + 4[(\gamma_{\alpha\beta} - \nu^{(3)}_{\alpha\beta})\Pi_{\alpha yz}
$$
$$
+ \nu^{(4)}_{\alpha\beta}\Pi_{\beta yz}]c_{\alpha z}c_{\alpha y} + \frac{4}{5}\sqrt{\frac{m_\alpha}{m}}\left[(\gamma_{\alpha\beta} - \nu^{(5)}_{\alpha\beta})q_\alpha\right.
$$
$$
+ \nu^{(6)}_{\alpha\beta}\sqrt{\frac{m_\beta}{m_\alpha}}q_\beta - \frac{5}{4}\nu^{(2)}_{\alpha\beta}(u_\alpha - u_\beta)\left]c_{\alpha z}\left(c_\alpha^2 - \frac{5}{2}\right)\right.
$$
$$
\tag{A1}
$$

for α, $\beta = 1, 2$. The $\gamma_{\alpha\beta}$ are proportional to the collision frequency between species α and β and they appear only in the combinations $\gamma_1 = \gamma_{11} + \gamma_{12}$ and $\gamma_2 = \gamma_{21} + \gamma_{22}$, where

$$
\gamma_\alpha = \frac{P_\alpha}{\mu_\alpha} = \frac{S_\alpha S_\beta - \nu^{(4)}_{\alpha\beta}\nu^{(4)}_{\beta\alpha}}{S_\beta + \nu^{(4)}_{\alpha\beta}},
\tag{A2}
$$

and

$$
S_\alpha = \nu^{(3)}_{\alpha\alpha} - \nu^{(4)}_{\alpha\alpha} + \nu^{(3)}_{\alpha\beta}.
\tag{A3}
$$

Note that the mixture viscosity is calculated via μ_α as $\mu = \mu_1 + \mu_2$. The explicit expressions of $\nu^{(i)}_{\alpha\beta}$ are as follows:

$$
\nu^{(1)}_{\alpha\beta} = \frac{16}{3}\frac{m_{\alpha\beta}}{m_\alpha}n_\beta\Omega^{(11)}_{\alpha\beta},
\tag{A4}
$$

$$
\nu^{(2)}_{\alpha\beta} = \frac{64}{15}\left(\frac{m_{\alpha\beta}}{m_\alpha}\right)^2 n_\beta\left(\Omega^{(12)}_{\alpha\beta} - \frac{5}{2}\Omega^{(22)}_{\alpha\beta}\right),
\tag{A5}
$$

$$
\nu^{(3)}_{\alpha\beta} = \frac{16}{5}\frac{m^2_{\alpha\beta}}{m_\alpha m_\beta}n_\beta\left(\frac{10}{3}\Omega^{(11)}_{\alpha\beta} + \frac{m_\beta}{m_\alpha}\Omega^{(22)}_{\alpha\beta}\right),
\tag{A6}
$$

$$
\nu^{(4)}_{\alpha\beta} = \frac{16}{5}\frac{m^2_{\alpha\beta}}{m_\alpha m_\beta}n_\beta\left(\frac{10}{3}\Omega^{(11)}_{\alpha\beta} - \Omega^{(22)}_{\alpha\beta}\right),
\tag{A7}
$$

$$
\nu^{(5)}_{\alpha\beta} = \frac{64}{15}\left(\frac{m_{\alpha\beta}}{m_\alpha}\right)^3\frac{m_\alpha}{m_\beta}n_\beta\left[\Omega^{(22)}_{\alpha\beta} + \left(\frac{15m_\alpha}{4m_\beta} + \frac{25}{8}\frac{m_\beta}{m_\alpha}\right)\Omega^{(11)}_{\alpha\beta}\right.
$$
$$
\left. - \frac{1}{2}\frac{m_\beta}{m_\alpha}(5\Omega^{(12)}_{\alpha\beta} - \Omega^{(13)}_{\alpha\beta})\right],
\tag{A8}
$$

$$
\nu^{(6)}_{\alpha\beta} = \frac{64}{15}\left(\frac{m_{\alpha\beta}}{m_\alpha}\right)^3\left(\frac{m_\alpha}{m_\beta}\right)^{3/2}n_\beta\left[-\Omega^{(22)}_{\alpha\beta} + \frac{55}{8}\Omega^{(11)}_{\alpha\beta} - \frac{5}{2}\Omega^{(12)}_{\alpha\beta}\right.
$$
$$
\left. + \frac{1}{2}\Omega^{(13)}_{\alpha\beta}\right],
\tag{A9}
$$

where

$$
m_{\alpha\beta} = \frac{m_\alpha m_\beta}{(m_\alpha + m_\beta)}.
\tag{A10}
$$

The $\Omega^{(kl)}_{\alpha\beta}$ are the Chapman–Cowling integrals.[13] For the realistic potential case they are calculated from the expressions given in Ref. 39.

Finally, starting from Eq. (20) for ω_α and using the definitions for the rarefaction parameter δ given by Eq. (13) as well as Eq. (A2) it is deduced that

$$
\omega_\alpha = \delta\left[\frac{C_0}{\gamma_1} + \frac{1 - C_0}{\gamma_2}\right]\sqrt{\frac{m_\alpha}{m}}.
\tag{A11}
$$

[1] C. M. Ho and Y. C. Tai, "Micro-electro-mechanical systems (MEMS) and fluid flows," Annu. Rev. Fluid Mech. **30**, 579 (1998).

[2] G. A. Bird, *Molecular Gas Dynamics and the Direct Simulation of Gas Flows* (Oxford University Press, Oxford, 1994).

[3] H. Xue, Q. Fan, and C. Shu, "Prediction of micro-channel flows using direct simulation Monte Carlo," Probab. Eng. Mech. **15**, 213 (2000).

[4] O. Aktas, N. R. Aluru, and U. Ravaioli, "Application of a parallel DSMC techique to predict flow characteristics in microfluidic filters," J. Microelectromech. Syst. **10**, 538 (2001).

[5] G. E. Karniadakis and A. Beskok, *Micro Flows. Fundamentals and Simulation* (Spinger, New York, 2001).

[6] E. B. Arkilic, M. A. Schmidt, and K. S. Breuer, "Gaseous slip flow in long microchannels," J. Microelectromech. Syst. **6**, 167 (1997).

[7] S. Colin, C. Aubert, and R. Caen, "Unsteady gaseous flows in rectangular microchannels: frequency response of one or two pneumatic lines connected in series," Eur. J. Mech. B/Fluids **17**, 79 (1998).

[8] F. Sharipov, "Application of the Cercignani–Lampis scattering kernel to calculations of rarefied gas flows. II. Slip and jump coefficients," Eur. J. Mech. B/Fluids **22**, 133 (2003).

[9] C. E. Siewert, "Viscous-slip, thermal-slip and temperature-jump coefficients as defined by the linearized Boltzmann equation and the Cercignani–Lampis boundary condition," Phys. Fluids **15**, 1696 (2003).

[10] T. Ohwada, Y. Sone, and K. Aoki, "Numerical analysis of the shear and thermal creep flows of a rarefied gas over a plane wall an the basis of the linearized Boltzmann equation for hard-sphere molecules," Phys. Fluids A **1**, 1588 (1989).

[11] S. K. Loyalka, "Temperature jump and thermal creep slip: Rigid sphere gas," Phys. Fluids A **1**, 403 (1989).

[12] S. Chapman and T. G. Cowling, *The Mathematical Theory of Non-Uniform Gases* (Cambridge University Press, Cambridge, 1952).

[13] J. H. Ferziger and H. G. Kaper, *Mathematical Theory of Transport Processes in Gases* (North-Holland, Amsterdam, 1972).

[14] C. Cercignani, *The Boltzmann Equation and Its Application* (Springer, New York, 1988).

[15] F. Sharipov and V. Seleznev, "Data on internal rarefied gas flows," J. Phys. Chem. Ref. Data **27**, 657 (1998).

[16] S. K. Loyalka, T. Storvick, and H. Park, "Poiseuille flow and thermal creep flow in long, rectangular channel in the molecular and transition flow regimes," J. Vac. Sci. Technol. **13**, 1188 (1976).

[17] F. Sharipov, "Rarefied gas flow through a long rectangular channel," J. Vac. Sci. Technol. A **17**, 3062 (1999).

[18] F. Sharipov, "Non-isothermal gas flow through rectangular microchannels," J. Micromech. Microeng. **9**, 394 (1999).

[19] V. G. Chernyak, V. V. Kalinin, and P. E. Suetin, "The kinetic phenomena in nonisothermal motion of a binary gas mixture through a plane channel," Int. J. Heat Mass Transfer **27**, 1189 (1984).

[20] Y. Onishi, "On the behaviour of a slightly rarefied gas mixture over plane boundaries," ZAMP **37**, 573 (1986).

[21] D. Valougeorgis, "Couette flow of a binary gas mixture," Phys. Fluids **31**, 521 (1988).

[22] F. Sharipov and D. Kalempa, "Gaseous mixture flow through a long tube at arbitrary Knudsen number," J. Vac. Sci. Technol. A **20**, 814 (2002).

[23] F. Sharipov and D. Kalempa, "Velocity slip and temperature jump coefficients for gaseous mixtures. I. Viscous slip coefficient," Phys. Fluids **15**, 1800 (2003).

[24] F. Sharipov and D. Kalempa, "Velocity slip and temperature jump coefficients for gaseous mixtures. II. Thermal slip coefficient," Phys. Fluids **16**, 759 (2004).

[25] F. Sharipov and D. Kalempa, "Velocity slip and temperature jump coefficients for gaseous mixtures. III. Diffusion slip coefficient," Phys. Fluids **16**, 3779 (2004).

[26] S. Naris, D. Valougeorgis, D. Kalempa, and F. Sharipov, "Gaseous mixture flow between two parallel plates in the whole range of the gas rarefaction," Physica A **336**, 294 (2004).

[27] C. E. Siewert and D. Valougeorgis, "The McCormack model: channel flow of a binary gas mixture driven by temperature, pressure and concentration gradients," Eur. J. Mech. B/Fluids **23**, 645 (2004).

[28] C. E. Siewert and D. Valougeorgis, "Concise and accurate solutions to half-space binary-gas flow problems defined by the McCormack model and specular-diffuse wall conditions," Eur. J. Mech. B/Fluids **23**, 709 (2004).

[29] F. J. McCormack, "Construction of linearized kinetic models for gaseous mixture and molecular gases," Phys. Fluids **16**, 2095 (1973).

[30] I. N. Ivchenko, S. K. Loyalka, and R. V. Tompson, "Boundary slip phenomena in a binary gas mixture," ZAMP **53**, 58 (2002).

[31] S. Takata, S. Yasuda, S. Kosuge, and K. Aoki, "Numerical analysis of thermal-slip and diffusion-slip flows of a binary mixture of hard-sphere molecular gases," Phys. Fluids **15**, 3745 (2003).

[32] S. Naris, D. Valougeorgis, F. Sharipov, and D. Kalempa, "Discrete velocity modelling of gaseous mixture flows in MEMS," Superlattices Microstruct. **35**, 629 (2004).

[33] D. Valougeorgis and S. Naris, "Acceleration schemes of the discrete velocity method: Gaseous flows in rectangular microchannels," SIAM J. Sci. Comput. (USA) **25**, 534 (2003).

[34] F. Sharipov, "Onsager–Casimir reciprocity relations for open gaseous systems at arbitrary rarefaction. I. General theory for single gas," Physica A **203**, 437 (1994).

[35] F. Sharipov, "Onsager–Casimir reciprocity relations for open gaseous systems at arbitrary rarefaction. II. Application of the theory for single gas," Physica A **203**, 457 (1994).

[36] F. Sharipov, "Onsager–Casimir reciprocity relations for open gaseous systems at arbitrary rarefaction. III. Theory and its application for gaseous mixtures," Physica A **209**, 457 (1994).

[37] E. E. Lewis and W. F. Miller, Jr., *Computational Methods in Neutron Transport Theory* (Wiley, New York, 1984).

[38] M. L. Adams and E. W. Larsen, "Fast iterative methods for discrete-ordinates particle calculations," Prog. Nucl. Energy **40**, 3 (2002).

[39] J. Kestin, K. Knierim, E. A. Mason, B. Najafi, S. T. Ro, and M. Waldman, "Equilibrium and transport properties of the noble gases and their mixture at low densities," J. Phys. Chem. Ref. Data **13**, 229 (1984).